Oncology Research, Vol. 27, pp. 945–956
Printed in the USA.

0965-0407/19 $90.00 + .00
DOI: https://doi.org/10.3727/096504019X15555408784978
E-ISSN 1555-3906
www.cognizantcommunication.com

Upregulation of Mobility in Pancreatic Cancer Cells by Secreted S100A11 Through Activation of Surrounding Fibroblasts

Yosuke Mitsui,*† Nahoko Tomonobu,* Masami Watanabe,† Rie Kinoshita,* I Wayan Sumardika,*‡ Chen Youyi,* Hitoshi Murata,* Ken-ichi Yamamoto,* Takuya Sadahira,† Acosta Gonzalez Herik Rodrigo,*† Hitoshi Takamatsu,* Kota Araki,*§ Akira Yamauchi,¶ Masahiro Yamamura,# Hideyo Fujiwara,** Yusuke Inoue,†† Junichiro Futami,‡‡ Ken Saito,§§ Hidekazu Iioka,§§ Eisaku Kondo,§§ Masahiro Nishibori,¶¶ Shinichi Toyooka,§ Yasuhiko Yamamoto,## Yasutomo Nasu,† and Masakiyo Sakaguchi*

*Department of Cell Biology, Okayama University Graduate School of Medicine, Dentistry and Pharmaceutical Sciences, Okayama, Japan
†Department of Urology, Okayama University Graduate School of Medicine, Dentistry and Pharmaceutical Sciences, Okayama, Japan
‡Faculty of Medicine, Udayana University, Denpasar, Bali, Indonesia
§Department of General Thoracic Surgery and Breast and Endocrinological Surgery, Okayama University Graduate School of Medicine, Dentistry and Pharmaceutical Sciences, Okayama, Japan
¶Department of Biochemistry, Kawasaki Medical School, Kurashiki, Okayama, Japan
#Department of Clinical Oncology, Kawasaki Medical School, Kurashiki, Okayama, Japan
**Department of Pathology, Kawasaki Medical School, Kurashiki, Okayama, Japan
††Faculty of Science and Technology, Division of Molecular Science, Gunma University, Kiryu, Gunma, Japan
‡‡Department of Interdisciplinary Science and Engineering in Health Systems, Okayama University, Okayama, Japan
§§Division of Molecular and Cellular Pathology, Niigata University Graduate School of Medical and Dental Sciences, Niigata, Japan
¶¶Department of Pharmacology, Okayama University Graduate School of Medicine, Dentistry and Pharmaceutical Sciences, Okayama, Japan
##Department of Biochemistry and Molecular Vascular Biology, Kanazawa University Graduate School of Medical Sciences, Kanazawa, Ishikawa, Japan

S100A11, a member of the S100 family of proteins, is actively secreted from pancreatic ductal adenocarcinoma (PDAC) cells. However, the role of the extracellular S100A11 in PDAC progression remains unclear. In the present study, we investigated the extracellular role of S100A11 in crosstalking between PDAC cells and surrounding fibroblasts in PDAC progression. An abundant S100A11 secreted from pancreatic cancer cells stimulated neighboring fibroblasts through receptor for advanced glycation end products (RAGE) upon S100A11 binding and was followed by not only an enhanced cancer cell motility in vitro but also an increased number of the PDAC-derived circulating tumor cells (CTCs) in vivo. Mechanistic investigation of RAGE downstream in fibroblasts revealed a novel contribution of a mitogen-activated protein kinase kinase kinase (MAPKKK), tumor progression locus 2 (TPL2), which is required for positive regulation of PDAC cell motility through induction of cyclooxygenase 2 (COX2) and its catalyzed production of prostaglandin E2 (PGE2), a strong chemoattractive fatty acid. The extracellularly released PGE2 from fibroblasts was required for the rise in cellular migration as well as infiltration of their adjacent PDAC cells in a coculture setting. Taken together, our data reveal a novel role of the secretory S100A11 in PDAC disseminative progression through activation of surrounding fibroblasts triggered by the S100A11–RAGE–TPL2–COX2 pathway. The findings of this study will contribute to the establishment of a novel therapeutic antidote to PDACs that are difficult to treat by regulating cancer-associated fibroblasts (CAFs) through targeting the identified pathway.

Key words: S100A11; Pancreatic cancer; Fibroblasts; RAGE; Cancer microenvironment

Address correspondence to Masakiyo Sakaguchi, Ph.D., Department of Cell Biology, Okayama University Graduate School of Medicine, Dentistry and Pharmaceutical Sciences, 2-5-1 Shikata-cho, Kita-ku, Okayama-shi, Okayama 700-8558, Japan. Tel: +81-86-235-7395; Fax: +81-86-235-7400; E-mail: masa-s@md.okayama-u.ac.jp

INTRODUCTION

Pancreatic ductal adenocarcinoma (PDAC), the most commonly observed type of pancreatic cancer, shows a highly aggressive phenotype even at an early stage, leading to poor survival[1,2]. One of the mechanisms responsible for its aggressiveness is derived from the renowned PDAC feature (i.e., frequent appearance of abundant stroma surrounding PDAC)[3,4]. The tumor stroma is composed of multiple noncancerous cell populations and extracellular matrix[3,5–8] with about 90% being occupied by fibroblasts[3,9]. Many scientists have therefore focused on the specific role of cancer-associated fibroblasts (CAFs) in the aggressive progression of PDAC. It has been reported that CAFs mediate metastasis[8,9], drug resistance[1], and immunosuppression[10]. Therefore CAFs may represent a critical target for anti-PDAC therapy. However, how CAFs are associated with PDAC aggressiveness at molecular levels has still not been fully elucidated.

Bearing in mind that as described above, we paid more attention on S100A11, which we have studied so far[4,11–17]. S100A11 is an EF-hand-type calcium-binding protein belonging to the S100 family of proteins[12]. It has become evident that S100A11 is overexpressed in PDAC, and its high level of expression is linked to poor survival[18]. We recently demonstrated that S100A11 is secreted from various kinds of cancer cells including PDAC cell lines at significant levels[11]. It has been shown that extracellular S100A11 provides cancer cells with increased ability for survival or mobility through receptor for advanced glycation end products (RAGE) in an autocrine manner[12,16,19]. We therefore considered the possibility that cancer-secreted S100A11 can also stimulate fibroblasts surrounding PDAC cells since RAGE is positively expressed in fibroblasts. The role(s) of extracellular S100A11 in fibroblasts and the possible relationship between S100A11-stimulated fibroblasts and cancer cells in PDAC progression have not been studied in detail.

Accordingly, in this study, we aimed to reveal the role of fibroblasts in PDAC with focus on the extracellular role of cancer-secreted S100A11.

MATERIALS AND METHODS

Cells

HEK293T cells (embryonic kidney cells stably expressing the SV40 large T antigen) and PK-8 cells (pancreatic carcinoma cells) were obtained from RIKEN BioResource Center (Tsukuba, Japan). Another human pancreatic cancer cell line, PANC-1, was obtained from ATCC (Manassas, VA, USA). Normal human OUMS-24 fibroblasts were established by Dr. Masayoshi Namba[20]. Wild-type (WT) and RAGE$^{-/-}$ mouse embryonic fibroblasts (MEFs) were provided by Professor Yasuhiko Yamamoto (Kanazawa University, Kanazawa, Japan). To stabilize the cell phenotype and avoid cellular senescence, the prepared primary mouse fibroblasts (WT and RAGE$^{-/-}$) were all immortalized in an autonomous manner through repeated passaging in cell culture[21]. These human and mouse cells were all cultivated in D/F medium (Thermo Fisher Scientific, Waltham, MA, USA) supplemented with 10% FBS.

Reagents

To selectively inhibit intrinsic kinase activities of TPL2 and ASK1, we used a TPL2 inhibitor (CAS 871307-18-5; Merck Millipore, Kenilworth, NJ, USA) and an ASK1 inhibitor [Selonsertib (GS-4997); Selleck, Osaka, Japan], respectively. Enzymatic activity of cyclooxygenase 2 (COX2) was suppressed by using a nonselective COX inhibitor, aspirin (Cayman Chemical, Ann Arbor, MI, USA), or two selective inhibitors of COX2, meloxicam (Cayman Chemical), and etodolac (Cayman Chemical). PGE2 was purchased from Cayman Chemical.

Human serum specimens from healthy donors [sample IDs: R297562 (age, 64 years; gender, female), R297571 (age, 35 years; gender, male), and R297604 (age, 56 years; gender, female)] and PDAC patients [sample IDs: 121229S (age, 39 years; gender, male; grade, G2; stage, IIA), 121230S (age, 47 years; gender, male; grade, G2; stage, IIA), and 121260S (age, 58 years; gender, male; grade, N/A; stage, IIB)] were purchased from Tennessee Blood Services (Memphis, TN, USA) and ProteoGenex (Inglewood, CA, USA), respectively. To measure concentrations of human S100A11 and PGEs in the serum specimens and cell culture media, ELISA kits for S100A11 (CircuLex S100A11 ELISA kit; CycLex, Nagano, Japan) and PGE2 (PGE2 high-sensitivity ELISA kit; Enzo Life Sciences, Farmingdale, NY, USA) were used. For in vivo mouse experiments, purified mouse IgG (Southern Biotech, Birmingham, AL, USA) was used as a control to the exRAGE-Fc decoy protein[22].

Recombinant Proteins

Highly purified human recombinant S100A11, S100A4, and S100A8/A9 proteins were prepared as reported previously[16,23]. The exRAGE-Fc decoy protein was prepared from its corresponding conditioned media from cultures of FreeStyle™ CHO-S cell (Chinese hamster ovary cell line; Thermo Fisher Scientific)-derived stable clone[22].

Expression Plasmids

To induce efficient expression of the transgenes in a temporal manner, we inserted cDNAs of interest into the pIDT-SMART (C-TSC) vector[24]. The prepared cDNAs were as follows: human cDNAs encoding RAGE and MAPK cascade upstream kinases (NAK, NIK, TAK1, DLK, TPL2, ASK1, SPRK, MLK1, MEKK3, LZK,

MLK4, and MKK5) and a kinase dead type of TPL2 (TPL2-KD; 167K replaced by M). RAGE was designed for expression as a C-terminal 3xHA-6His-tagged form. MAPK cascade upstream kinases and TPL2-KD were designed for expression as C-terminal Myc-6His-tagged forms. Cells were transiently transfected with the plasmid vectors using FuGENE-HD (Promega, Madison, WI, USA).

To obtain PK-8 clones that exhibit a significantly high expression level of a foreign gene, GFP alone, or GFP+S100A11, in a stable manner, individual *GFP* and *S100A11* cDNAs were inserted into the pSAKA-4B vector[22,25]. Using the resulting expression constructs, pSAKA-4B-GFP and pSAKA-4B-S100A11, GFP- and GFP+S100A11-overexpressed clones were established from PK-8 parental cells through a convenient electroporation gene delivery method and following selection with puromycin at 20 μg/ml.

Cellular Migration and Invasion Assays in a Boyden Chamber

Evaluations of in vitro cellular migration and invasion were followed by a convenient Boyden chamber method set with Matrigel-noncoating (for migration) or -coating Transwell membrane (for invasion). To study the contribution of fibroblasts to cancer cell migration, we seeded OUMS-24 normal human fibroblasts (5×10^4 cells/well) on the bottom chamber and filled the chamber with 0.5% FBS low-serum medium. Before seeding PDAC cells on the top chamber, OUMS-24 cells on the bottom chamber were treated or not treated with recombinant S100A11 (100 ng/ml) in the presence or absence of exRAGE-Fc (1 μg/ml). After setting PK-8 or PANC-1 cells (5×10^4 cells/insert) on the upper chamber, an additional 24-h incubation was done to assess fibroblast tropic migration of PDAC cells.

Another migration assay was also performed by a method similar to that described above. In this setting, PK-8 cell sublines (PK-8 GFP or PK-8 GFP/A11, 5×10^4 cells/well) and mouse fibroblasts (WT or RAGE$^{-/-}$, 5×10^4 cells/well) were simultaneously seeded in various combinations between PK-8 cell sublines and mouse fibroblasts in the same upper chamber filled with low-serum medium (0.5% FBS), and the lower chamber was also filled with 0.5% FBS low-serum medium. After 24 h, migrating cells with GFP on the underside of inserts were imaged under a fluorescent microscope (BZ-9000; Keyence, Tokyo, Japan). All the migrated GFP$^+$ cells that migrated were counted by fluorescence-based scanning (Fluoroskan Ascent FL; Thermo Fisher Scientific).

Western Blot Analysis

Western blot analysis was performed under conventional conditions. The antibodies used were rabbit anti-COX2 antibody (Cell Signaling Technology, Beverly, MA, USA), mouse anti-tubulin antibody (Sigma-Aldrich, St. Louis, MO, USA), and mouse anti-Myc antibody (Cell Signaling Technology). Agarose beads conjugated with monoclonal anti-HA tag antibody (Sigma-Aldrich) and monoclonal anti-Myc tag antibody (MBL, Nagoya, Japan) were used for coimmunoprecipitation experiments.

Mouse PDAC Model and its Evaluations

PK-8 cells (parental or PK-8 GFP clone, 2×10^6 cells or 3×10^6 cells) were subcutaneously transplanted into the back right side of BALB/c nu/nu mice (SLC, Hamamatsu, Japan) in either a single or mixed condition with the same number of normal human OUMS-24 fibroblasts (2×0^6 cells or 3×10^6 cells). The size of tumors was measured with a vernier caliper, and tumor volume was calculated as $1/2\times(\text{shortest diameter})^2\times(\text{longest diameter})$. After the tumor had grown at the injected site to 4–5 mm in diameter, either control IgG (100 μg/100 μl/mouse) or exRAGE-Fc (100 μg/100 μl/mouse) was subcutaneously administered into the back on the left side (nontumor area) of each mouse six times at constant 1-week intervals (on days 3, 10, 17, 24, 31, and 38) for 44 days.

To count circulating tumor cells (CTCs) in the tumor-bearing mice, 500 μl of whole blood was obtained from each mouse. The collected blood specimens were supplemented with EDTA (final concentration 1 mg/ml), treated with 1.5 μl of red blood cell lysis buffer (Roche, Basel, Switzerland), and stained with APC-conjugated anti-CD45 antibody (BioLegend, San Diego, CA, USA), which is useful for distinguishing GFP-labeled cells (CTCs) from an abundant leukocyte population in the analytic image of flow cytometry. The treated specimens were then subjected to flow cytometric analysis to count CTCs. Flow cytometry was performed on a MACS Quant Analyzer (Miltenyi Biotec GmbH, Bergisch Gladbach, Germany) using MACS Quantify Software Ver. 2.5 (Miltenyi Biotec GmbH). Data were analyzed using FlowJo software (FlowJo, LLC; BD Biosciences, Franklin Lakes, NJ, USA).

Statistical Analysis

Data are expressed as means ± SD. We employed simple pairwise comparison with Student's *t*-test (two-tailed distribution with two-sample equal variance). A value of $p<0.05$ was considered significant.

RESULTS AND DISCUSSION

We previously reported that S100A11 is markedly upregulated in PDAC cell lines at not only the intracellular level but also the secreted extracellular level[21]. The active secretion of S100A11 from PDAC cell lines were also observed in clinical PDACs specimens since we found that S100A11 exhibits a tendency to increase in

serum from PDAC patients compared to that in serum from healthy donors (data not shown). Our recent work demonstrated that extracellular S100A11 secreted from PDAC cells significantly activates proliferation of adjacent fibroblasts but not PDAC cells via RAGE on the surface of fibroblasts, resulting in fertilization of PDAC stroma, which in turn enforces tumor progression in vivo[21]. In this experimental setting, we found that growth and motility of PDAC cells are pronouncedly upregulated by unidentified soluble factors secreted from S100A11-stimulated fibroblasts. In this study, we therefore aimed to identify the soluble factor(s).

At first, in order to confirm the fibroblast role in tumor toward tumor progression in vivo, we transplanted PK-8 cells (a human PDAC cell line) alone or PK-8 cells mixed with human fibroblasts (OUMS-24 cells) into the subcutaneous area of nude mice. As shown in Figure 1A and B, both tumor volume and weight were much larger in the group transplanted with mixed population of cells than in the group transplanted with only PK-8 cells. To examine how S100A11 contributes to tumor progression with crosstalking between PDAC cells and fibroblasts, the behavior of PK-8 cells was examined under the presence of a condition medium (CM) from S100A11 (100 ng/ml)-stimulated OUMS-24 fibroblasts in a culture system [Supplementary Fig. 1A (growth) and B (migration), available at https://www.dropbox.com/sh/58jtq8girxm80aw/AAA60uI3KPCPPkJ0x1JfG8O6a?dl=0]. By this approach, we found that the CM from fibroblasts has the ability to greatly increase either proliferation (Supplementary Fig. 1C) or migration (Fig. 1C) of PK-8 cells. Interestingly, although the upregulated growth of PK-8 cells with the nontreated fibroblast CM was not positively affected by the CM from S100A11-stimulated fibroblasts (Supplementary Fig. 1C), the increased ability of PK-8 cells for migration was further enhanced by the S100A11-treated fibroblast CM (Fig. 1C). In this experimental setting, we confirmed that (1) S100A11 recombinant protein alone set in the bottom chamber had no effect on PK-8 cell motility without fibroblasts (data not shown), (2) much higher doses (500 and 1,000 ng/ml) of S100A11 did not result in further enhancement of migration activity in PK-8 cells through fibroblasts (Supplementary Fig. 1D), and (3) S100A11 showed the highest activity for PK-8 cell migration in this coculture context among the cancer-relevant S100 proteins (S100A4, S100A8/A9, a heterodimer complex composed of S100A8 and S100A9, and S100A11) at 100 ng/ml (Supplementary Fig. 1E).

The increased motility with S100A11 was also seen in another PDAC cell line, PANC-1 (Fig. 1D). The exRAGE-Fc decoy that prevents S100A11 binding to intrinsic RAGE through capturing extracellular S100A11[22] reduced the enhanced migration of PK-8 cells by the S100A11-treated fibroblast CM (Fig. 1E), suggesting an important role of the S100A11–RAGE axis in fibroblasts for inducing a soluble factor(s) that activates PDAC cell motility. In this experimental setting, we also found that the basal migration ability of PK-8 cells caused by the nonstimulated fibroblast CM is reduced by treatment with exRAGE-Fc. This may be explained by the contribution of a RAGE ligand other than S100A11. Since S100A11 is not secreted from fibroblasts[21], we speculated that an unidentified RAGE ligand(s) secreted from fibroblasts cooperatively functions with S100A11 from PDAC cells to induce a certain PDAC chemoattractant(s) through RAGE on fibroblasts.

In a physiological condition, fibroblasts are attached to cancer cells in a PDAC tumor. We therefore cocultured PK-8 cells with WT mouse fibroblasts (WT fibroblasts) or RAGE KO mouse fibroblasts (RAGE$^{-/-}$ fibroblasts)[21] and examined the migration activity of PK-8 cells under the mixed condition (Supplementary Fig. 2A, available at https://www.dropbox.com/sh/58jtq8girxm80aw/AAA60uI3KPCPPkJ0x1JfG8O6a?dl=0). To distinguish PK-8 cells from fibroblasts in migration activity, we labeled PK-8 cells with green fluorescence protein (GFP) by a chromosomal insertion of the *GFP* gene expression unit that enables PK-8 cells to express GFP protein in a stable manner, resulting in creation of a control subline PK-8 GFP clone (PK-8 GFP). At that time, to examine the effect of extracellular S100A11 on the mixed culture, we established an additional PK-8 subline (PK-8 GFP/A11) that stably expresses an abundant S100A11 other than GFP. We confirmed that the secretion level of S100A11 in PK-8 GFP/A11 cells was about fivefold higher than that in PK-8 parental cells (Fig. 1F). Although PK-8 GFP cells did not show migration and invasion activities in the absence of WT fibroblasts (data not shown), we found that migration and invasion were both induced in PK-8 GFP cells by cocultivation with WT fibroblasts and that these activities were further increased in PK-8 GFP/A11 cells [Fig. 1G and Supplementary Figs. 2B (migration) and 1H (invasion)]. The upregulations were both in turn mitigated when the PK-8 sublines were mixed with RAGE$^{-/-}$ fibroblasts, suggesting a crucial role of the S100A11–RAGE axis in fibroblasts for activating invasive motility of PDAC cells. In these experimental settings, the increased activities of migration and invasion caused by S100A11 overexpression were not diminished to the basal migration level of control PK-8 GFP cells. This is probably due to the presence of another S100A11 receptor(s) that is similar to RAGE in composition. We have reported RAGE-like receptors including melanoma cell adhesion molecule (MCAM), activated leukocyte cell adhesion molecule (ALCAM), extracellular matrix metalloproteinase inducer (EMMPRIN), and neuroplastin (NPTN)[26–28]. These receptors react with other S100 family proteins including S100A8/A9, a heterodimer

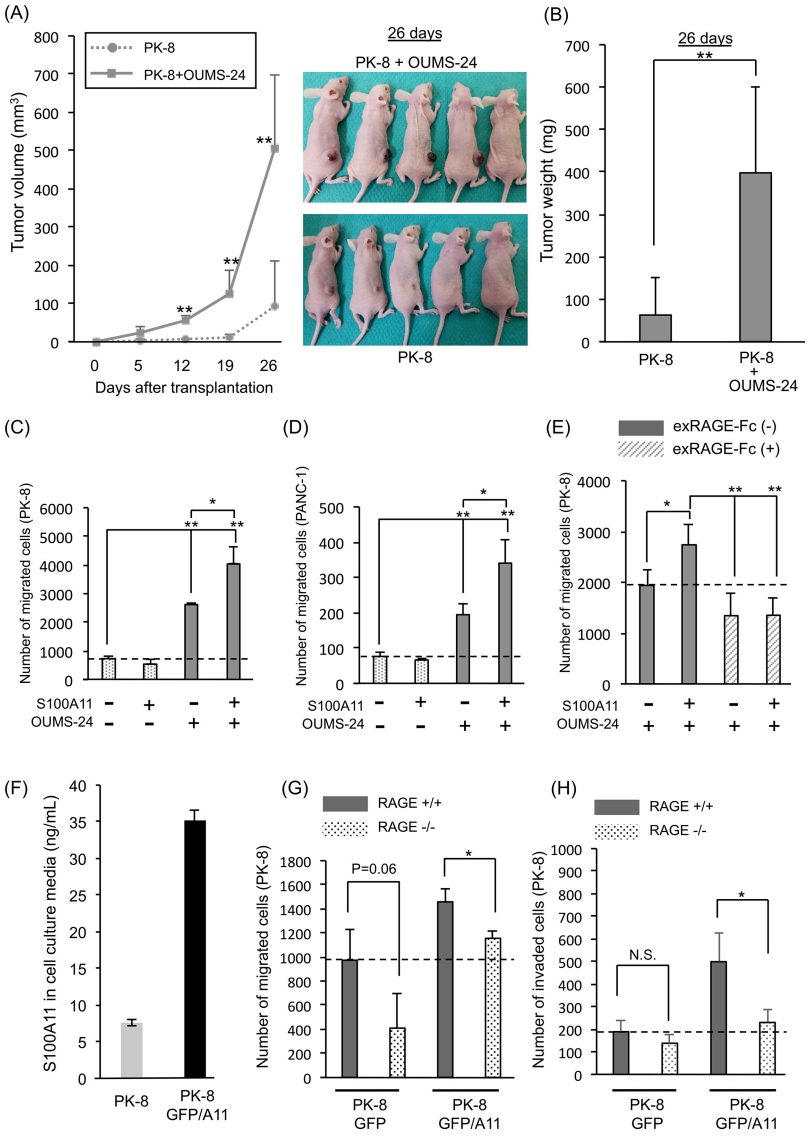

Figure 1. Effect of fibroblasts on pancreatic ductal adenocarcinoma (PDAC) progression through the S100A11–receptor for advanced glycation end products (RAGE) axis. (A) Tumor sizes were monitored on the indicated days after transplantation of the prepared cells [pancreatic carcinoma cells (PK-8 cells) alone (2×10^6 cells), PK-8 cells (2×10^6 cells) + normal human OUMS-24 fibroblasts (2×10^6 cells)]. OUMS-24 fibroblasts showed no tumorigenesis when they were subcutaneously injected into nude mice as a single-cell population (data not shown). (B) Tumor weights were quantified 26 days after transplantation. (C–E) A migration assay was performed by the Boyden chamber method. PK-8 cells (C, E) and PANC-1 cells (D) were seeded on the top chambers to be 5×10^4 cells/chamber. OUMS-24 fibroblasts (5×10^4 cells) were set on each bottom chamber to constantly supply the fibroblast-conditioned medium. OUMS-24 fibroblasts in the bottom chamber were then stimulated (+) or not stimulated (−) with S100A11 at a final concentration of 100 ng/ml (C–E). (E) To prevent S100A11–RAGE interaction on OUMS-24 fibroblasts, exRAGE-Fc (1.0 μg/ml) was also added to the same bottom chamber. Cancer cell migration was assessed at 24 h after setting of the assay (C–E). (F) The secretion level of S100A11 from a PK-8 GFP/A11 stable clone was evaluated by monitoring S100A11 in its cultured medium with ELISA in comparison to that from parental PK-8 cells. (G, H) A GFP-labeled PK-8 clone (PK-8 GFP or PK-8 GFP/A11) (5×10^4 cells) was mixed with mouse WT fibroblasts or mouse RAGE$^{-/-}$ fibroblasts and placed on the top chamber (see Supplementary Fig. 2A). Twenty-four hours after cultivation, the PK-8 cells that had migrated (G) or invaded (H) were monitored by the expressed GFP color. The graphs show quantified data of migration (G) and invasion (H) events. Data are means ± SD; N.S., not significant; *$p<0.05$ and **$p<0.01$.

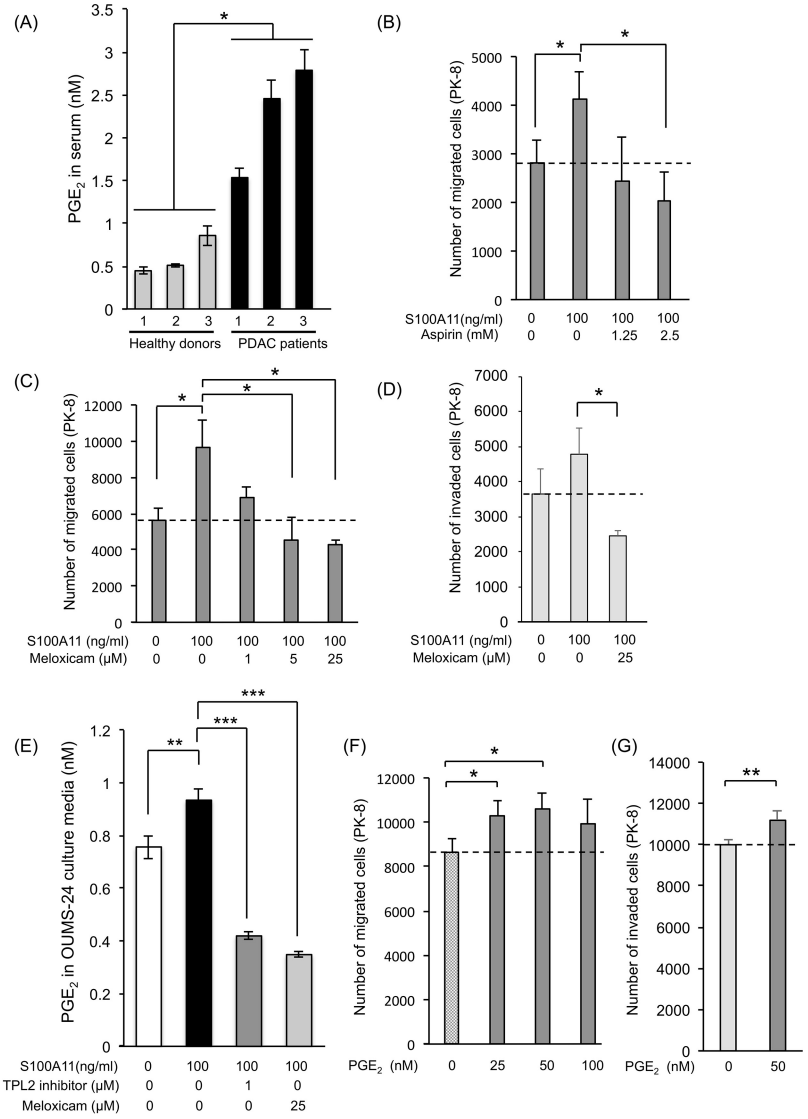

Figure 2. Significant role of prostaglandin E2 (PGE2) in upregulation of PDAC cell migration induced by the S100A11–RAGE axis in fibroblasts. (A) PGE2 levels in sera collected from PDAC patients were monitored and quantified by ELISA. (B, C) In vitro migration of PK-8 cells was evaluated by a method similar to that described in the legend of Figure 1E except for the use of cyclooxygenase (COX) inhibitors, aspirin (inhibitor of COX1 and COX2, B) and meloxicam (selective inhibitor of COX2, C) in the bottom chamber in which fibroblasts were present. (D) Cellular invasion of PK-8 cells was also evaluated by a method similar to that described above (C) except for the use of Matrigel-covered membrane set in the Transwell chamber. (E) Culture media of OUMS-24 fibroblasts were collected after treatment of the cells with S100A11 (100 ng/ml, 24 h) in the presence or absence of a tumor progression locus 2 (TPL2) inhibitor or meloxicam. The culture media were then subjected to ELISA to monitor the PGE2 levels in the media. (F, G) Migration (F) and invasion (G) assays were performed using a Boyden chamber. PK-8 cells (5×10^4 cells) were set in the top chamber, and PGE2 was added to the bottom chamber without fibroblasts. PK-8 cell migration was assessed at 24 h after addition of PGE2 to 10% FBS medium set in the bottom chamber. Data are means ± SD. *$p<0.05$, **$p<0.01$, ***$p<0.001$.

complex composed of S100A8 and S100A9. Our RNA-seq data demonstrated that MCAM alone was elevated among the receptors at a significant level when RAGE was knocked out in mouse fibroblasts[21]. We hence considered that MCAM may function as a compensatory receptor to S100A11 in fibroblasts to maintain cellular homeostasis, and this issue about the interaction of S100A11 with MCAM and its physiological role in the cancer microenvironment is part of our ongoing study.

In order to obtain a mechanistic clue regarding the positive regulation of cancer motility by activated fibroblasts through the S100A11–RAGE axis, we performed comparative analysis of gene expression, with focus on genes encoding soluble secretory proteins, in

mouse WT fibroblasts treated with and not treated with S100A11. However, unexpectedly, the results of RNA-seq analysis showed that there were no appreciable differences in gene expression (data not shown). We then examined the alteration of gene expression in mouse WT fibroblasts compared to that in mouse RAGE$^{-/-}$ fibroblasts and found that several cancer-related soluble factors were downregulated in mouse RAGE$^{-/-}$ fibroblasts (Supplementary Fig. 3A, available at https://www.dropbox.com/sh/58jtq8girxm80aw/AAA60uI3KPCPPkJ0x1JfG8O6a?dl=0). Among the altered genes, we selected genes that are highly relevant to cancer progression (highlighted by red color)[29–34]. Their downregulation that happened in concomitant to RAGE KO was confirmed by the quantitative real-time PCR technique (Supplementary Fig. 3B). However, the expression levels of the altered genes of interest were not enhanced by treatment with S100A11 in mouse WT fibroblasts (Supplementary Fig. 4A, available at https://www.dropbox.com/sh/58jtq8girxm80aw/AAA60uI3KPCPPkJ0x1JfG8O6a?dl=0) or in human OUMS-24 fibroblasts except for a subtle increase in matrix metalloproteinase MMP13 (Supplementary Fig. 4B). These negative results spurred us next to focus on another candidate, fatty acids, which act as powerful cancer chemoattractants. It has long been recognized that prostaglandin E2 (PGE2) plays an unusual role in cancer growth and metastasis,[35] and PGE2 was actually upregulated in serum from PDAC patients (Fig. 2A). We hence tried to examine the role of PGE2 in PDAC by suppressing the production of PGE2 in fibroblasts using cyclooxygenase (COX) inhibitors (aspirin: inhibitor of COX1 and COX2, meloxicam and etodolac: selective inhibitor of COX2). As shown in Figure 2B and C and Supplementary Figures 5 (migration) and 2D (invasion) (available at https://www.dropbox.com/sh/58jtq8girxm80aw/AAA60uI3KPCPPkJ0x1JfG8O6a?dl=0), these inhibitors effectively eliminated the activation force of S100A11-stimulated fibroblasts, resulting in the reduction of both migration and invasion of PK-8 cells in a dose-dependent manner without apoptotic cell death in the treated fibroblasts. In parallel with this, we confirmed that meloxicam effectively suppressed PGE2 production in human OUMS-24 fibroblasts (Fig. 2E). In addition, we found that extracellular PGE2 at 25 nM is sufficient to stimulate the migration of PK-8 cells, and the treatment at 50 nM shows the highest induction of the migration (Fig. 2F). We also confirmed that 50 nM of PGE2 is enough to activate an invasive movement of PK-8 cells (Fig. 2G). One reason for cellular migration requiring higher concentration (25 nM) than the physiological concentration induced by S100A11 is probably deterioration of the stocked PGE2 reagent since unsaturated fatty acids are rapidly inactivated by oxidization. Endogenous fresh PGE2 may have higher activity than that of the stocked one. Collectively, the results suggest an important role of fibroblast-mediated secretory PGE2 in positive regulation of PDAC cell motility, which is triggered by the S100A11–RAGE–COX2 axis in fibroblasts.

Our next interest was how PGE2 is induced by RAGE upon S100A11 binding. To examine a RAGE downstream signal that is required for COX2 activation and subsequent production of PGE2, we attempted to identify a signal upstream kinase as a novel binding partner to RAGE that may trigger the signal onset of RAGE in the cytoplasm. Each of the mitogen-activated protein kinase kinase kinases (MAPKKKs: NAK, NIK, TAK1, DLK, TPL2, ASK1, SPRK, MLK1, MEKK3, LZK, and MLK4) and MAPKK (MKK5) was cotransfected with RAGE in HEK293T cells, and their interactions were studied by an immunoprecipitation (IP) technique. By this approach, we found novel interactions of RAGE with TPL2 and ASK1 (Fig. 3A). Given that these interactions are important to induce PGE2 production, we asked the significance of the recruitment of the kinases to RAGE in activation of COX2 in fibroblasts. Interestingly, functional inhibition of TPL2, but not that of ASK1, reduced either the S100A11-mediated induction of COX2 (Fig. 3B) or PGE2 (Fig. 2E) in OUMS-24 fibroblasts at a pronounced level. Both a TPL2 inhibitor (Fig. 3C) and overexpression of a kinase-dead type of TPL2 (TPL2-KD) (Supplementary Fig. 6, available at https://www.dropbox.com/sh/58jtq8girxm80aw/AAA60uI3KPCPPkJ0x1JfG8O6a?dl=0) also markedly attenuated the ability of fibroblasts to induce upregulation of PK-8 cell motility with the help of S100A11. These results indicate a crucial role of the S100A11–RAGE–COX2–PGE2 axis in fibroblasts for PDAC progression with increased motility of adjacent cancer cells. A linkage between TPL2 and COX2 was also reported in macrophages in response to a lipopolysaccharide (LPS)[35]. In that study, it was revealed that regulation of COX2 by TPL2 depends on the ERK-MAPK (ERK) and p38-MAPK (p38) pathways, which activate CREB, a critical enhancer of COX2 transcription. A similar mechanism may function in the RAGE downstream in fibroblasts upon S100A11 binding since we also detected increased phosphorylation of ERK2, but not that of ERK1, or p38 for all of its isoforms (p38a, b, d, and g) (Supplementary Fig. 7, available at https://www.dropbox.com/sh/58jtq8girxm80aw/AAA60uI3KPCPPkJ0x1JfG8O6a?dl=0).

Last, we extended our research to an animal model for PDAC progression with increased cell motility of cancer cells. In order to confirm the important role of RAGE in cancer-associated fibroblasts for tumor growth and cancer cell motility, we subcutaneously transplanted a mixture of PK-8 cells and OUMS-24 fibroblasts and evaluated their growth (Fig. 4A and B) and cancer cell motility (Fig. 4C) after injection of either control IgG or exRAGE-Fc. In this experimental setting, cancer cell

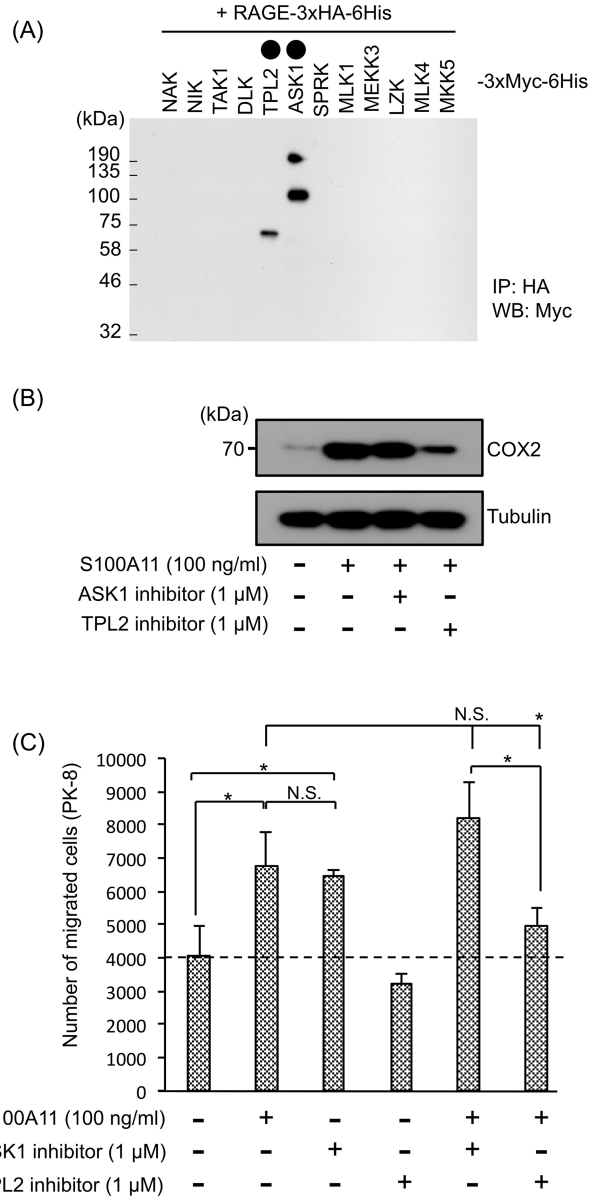

Figure 3. Significant role of TPL2 in induction of COX2 through S100A11–RAGE interaction in fibroblasts, which greatly contributes to the upregulation of PDAC cell migration caused by S100A11-stimulated fibroblasts. (A) HEK293T cells were cotransfected with HA-tagged RAGE and each of the indicated Myc-tagged upstream kinases, NAK (NF-kB-activating kinase: *TBK1*), NIK (NF-kB-inducing kinase: *MAP3K14*), TAK1 (TGF-b activated kinase 1: *MAP3K7*), DLK (dual leucine zipper-bearing kinase: *MAP3K12*), TPL2 (*MAP3K8*), ASK1 (apoptosis signal-regulating kinase 1: *MAP3K5*), SPRK (Src-homology 3 domain-containing proline-rich kinase: *MAP3K11*), MLK1 (mixed lineage kinase 1: *MAP3K9*), MEKK3 (MAPK/ERK kinase kinase 3: *MAP3K3*), LZK (leucine zipper-bearing kinase: *MAP3K13*), MLK4 (mixed lineage kinase 4: *MAP3K21*), and MKK5 (MAP kinase kinase 5: *MAP2K5*). After immunoprecipitation of the expressed RAGE with HA antibody-conjugated beads, kinases that interacted were detected by Myc antibody. Circles painted black show the candidates that interacted with RAGE. (B) COX2 induction was monitored in OUMS-24 fibroblasts by Western blotting. OUMS-24 fibroblasts were treated or not treated with S100A11 (100 ng/ml, 24 h) in the presence or absence of the indicated inhibitors (ASK1 inhibitor and TPL2 inhibitor). (C) A migration assay was performed by a method similar to that described in the legend of Figure 2B–D except for the use of different inhibitors (ASK1 inhibitor and TPL2 inhibitor). Data are means ± SD. N.S., not significant; $*p<0.05$.

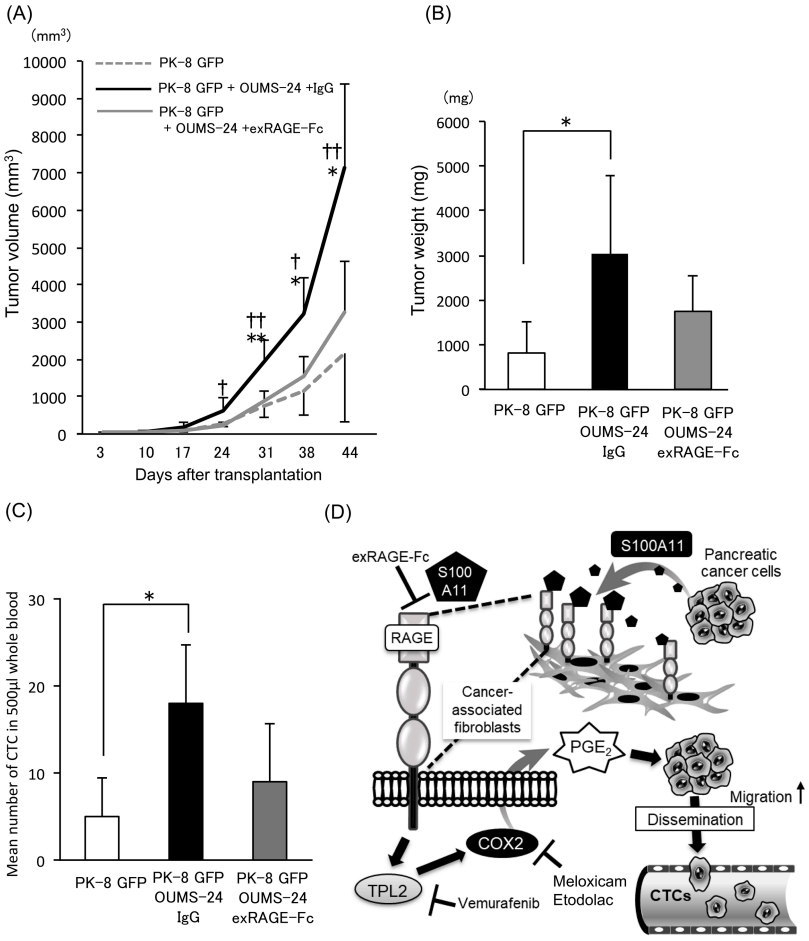

Figure 4. Effect of exRAGE-Fc on PDAC progression in vivo. (A) Tumor sizes were monitored on the indicated days after transplantation of the prepared cells [PK-8 GFP cells alone (3×10^6 cells), PK-8 GFP cells (3×10^6 cells)+OUMS-24 fibroblasts (3×10^6 cells)]. Mice that were injected with the mixed cells (PK-8 GFP/OUMS-24) were treated with either control IgG (100 µg/100 µl/mouse) or exRAGE-Fc (100 µg/100 µl/mouse) six times at constant 1-week intervals (on days 3, 10, 17, 24, 31, and 38) for 44 days. Data are means±SD. *$p<0.05$, **$p<0.01$ (PK-8 GFP+OUMS-24+exRAGE-Fc vs. PK-8 GFP+OUMS-24+IgG) or †$p<0.05$ and ††$p<0.01$ (PK-8 GFP+OUMS-24+exRAGE-Fc vs. PK-8 GFP). (B) Tumor weights were quantified 44 days after transplantation. Data are means±SD. *$p<0.05$. (C) After 44 days of the tumor monitoring, PK-8 GFP clone-derived circulating tumor cells (CTCs) from the indicated three groups were evaluated by flow cytometry using collected mouse whole blood specimens (500 µl/mouse). The gated GFP^+ cell populations are quantified, and the resulting data that express cell numbers are shown by bar graphs. Data are means±SD. *$p<0.05$. (D) The schematic shows a reaction model of the identified pathway that plays a crucial role in PDAC progression through crosstalking between PDAC cells and adjacent fibroblasts, leading to an increased level of CTCs, which may greatly contribute to the increase in metastatic aggressiveness of PDAC.

motility was assessed by monitoring the number of circulating tumor cells (CTCs) since we confirmed that PK-8 cells never showed aggressive metastatic behavior to distant organs such as the lung, liver, and brain from the subcutaneous primary tumor area even when mixed with fibroblasts (data not shown). However, given that migration activity of PK-8 cells is highly elevated at the primary tumor area by fibroblasts, some cells will actively disseminate and enter the blood stream as CTCs. As a result, we found that tumor volume (Fig. 4A), tumor weight (Fig. 4B), and number of CTCs (Fig. 4C) were all markedly elevated in the group with a mixed tumor (PK-8 GFP cells and OUMS-24 fibroblasts) compared to those in the group with a tumor derived from only PK-8 GFP cells. Treatment of the mixed tumor with exRAGE-Fc tended to suppress tumor growth and decrease the number of CTCs. These results suggest that RAGE in fibroblasts contributes to an increase in the number of CTCs as well as tumor growth in an in vivo situation (Fig. 4D).

Here we could not yet be sure at the time that although PDAC patients have increased PGE2 levels in their sera compared with those in healthy donors as shown in Figure 2A, S100A11–RAGE–TPL2–COX2 axis in fibroblasts

actually functions to upregulate PGE2 in the patient's living body. In this issue, Xie et al. reported the rise in the concentration of PGE2 in PDAC-bearing mice, in which tumor-induced elevation of PGE2 (around 70 pg/mg) was reduced to around 30 pg/mg by a COX2 inhibitor[36]. It also followed that COX2 inhibitor efficiently blocked tumor progression in the mouse xenograft model of PDAC. This implies an important role of COX2-mediated PGE2 production in PDAC progression in vivo. We hence support the idea that our identified S100A11–RAGE–TPL2 axis contributes in part to the activation of COX2, which in turn induces PGE2 in vivo.

As already explained, a RAGE ligand is not restricted to S100A11. Various ligands are present in an in vivo environment (living body) rather than in an in vitro environment (cell culture system). We hence considered the possibility that several other ligands in a living body other than PK-8 cell-derived S100A11 bind to RAGE on cancer neighboring fibroblasts, resulting in production of several soluble proteins (Supplementary Fig. 3B) that may greatly contribute to cancer growth with a mutual cooperation among them. On the other hand, we revealed that S100A11 from PDAC cells induces the production of soluble fatty acid PGE2 in cancer-associated fibroblasts through activation of the RAGE–TPL2–COX2 pathway, which in turn can activate PDAC motility, eventually leading to an increase in the number of CTCs in in vivo situation. In this experimental setting, exRAGE-Fc resulted in showing a tendency to suppress tumor growth (Fig. 4B) as well as showing a tendency to reduce the number of CTCs (Fig. 4C), but both suppressive effects were not significant. These results may be explained by the presence of receptors similar to RAGE such as MCAM in fibroblasts since MCAM may be upregulated by suppression of RAGE as cellular compensatory machinery even in an in vivo situation[21]. Further studies are required to elucidate these elaborate mechanisms.

CONCLUSION

In this study, we revealed an unusual role of fibroblasts in upregulation of PDAC cell motility that requires certain crosstalking between PDAC cells and surrounding fibroblasts in the cancer stroma through PDAC cell-secreted S100A11 and its receptor RAGE on fibroblasts. In this context, we found that PGE2, which is induced by the S100A11–RAGE–TPL2–COX2 axis in fibroblasts, functions as a key soluble factor to accelerate PDAC cell motility, resulting in an increased number of CTCs in vivo. In addition, we found that RAGE in fibroblasts also contributes to the upregulation of PDAC growth in vivo. Thus, the establishment of a strategy for targeting the S100A11–RAGE–TPL2–COX2 pathway in CAFs in PDAC may provide an advanced benefit for a therapeutic approach for PDACs that are difficult to treat. In fact, exRAGE-Fc showed a tendency to suppress PDAC growth and reduce the concomitant increase in the number of CTCs in vivo.

ACKNOWLEDGMENTS: This work was supported by the Foundation for Promotion of Cancer Research (M. Sakaguchi) and in part by grants from the JSPS KAKENHI Grant (No. 17H03577) (M. Sakaguchi), JSPS KAKENHI Grant (No. 18H02937) (Y. Nasu), JSPS KAKENHI Grant (No. 15K10201) (A. Yamauchi), and Takeda Science Foundation (M. Sakaguchi). The authors declare no conflicts of interest.

REFERENCES

1. Aslan M, Shahbazi R, Ulubayram K, Ozpolat B. Targeted therapies for pancreatic cancer and hurdles ahead. Anticancer Res. 2018;38(12):6591–606.
2. Keleg S, Buchler P, Ludwig R, Buchler MW, Friess H. Invasion and metastasis in pancreatic cancer. Mol Cancer 2003;2:14.
3. von Ahrens D, Bhagat TD, Nagrath D, Maitra A, Verma A. The role of stromal cancer-associated fibroblasts in pancreatic cancer. J Hematol Oncol. 2017;10(1):76.
4. Saito K, Sakaguchi M, Maruyama S, Iioka H, Putranto EW, Sumardika IW, Tomonobu N, Kawasaki T, Homma K, Kondo E. Stromal mesenchymal stem cells facilitate pancreatic cancer progression by regulating specific secretory molecules through mutual cellular interaction. J Cancer 2018;9(16):2916–29.
5. Zhang A, Qian Y, Ye Z, Chen H, Xie H, Zhou L, Shen Y, Zheng S. Cancer-associated fibroblasts promote M2 polarization of macrophages in pancreatic ductal adenocarcinoma. Cancer Med. 2017;6(2):463–70.
6. Shan T, Chen S, Chen X, Lin WR, Li W, Ma J, Wu T, Cui X, Ji H, Li Y, Kang Y. Cancer-associated fibroblasts enhance pancreatic cancer cell invasion by remodeling the metabolic conversion mechanism. Oncol Rep. 2017; 37(4):1971–9.
7. Bolm L, Cigolla S, Wittel UA, Hopt UT, Keck T, Rades D, Bronsert P, Wellner UF. The role of fibroblasts in pancreatic cancer: Extracellular matrix versus paracrine factors. Transl Oncol. 2017;10(4):578–88.
8. Hwang RF, Moore T, Arumugam T, Ramachandran V, Amos KD, Rivera A, Ji B, Evans DB, Logsdon CD. Cancer-associated stromal fibroblasts promote pancreatic tumor progression. Cancer Res. 2008;68(3):918–26.
9. Xing F, Saidou J, Watabe K. Cancer associated fibroblasts (CAFs) in tumor microenvironment. Front Biosci. (Landmark Ed) 2010;15:166–79.
10. Yang X, Lin Y, Shi Y, Li B, Liu W, Yin W, Dang Y, Chu Y, Fan J, He R. FAP promotes immunosuppression by cancer-associated fibroblasts in the tumor microenvironment via STAT3-CCL2 signaling. Cancer Res. 2016;76(14):4124–35.
11. Saho S, Satoh H, Kondo E, Inoue Y, Yamauchi A, Murata H, Kinoshita R, Yamamoto K, Futami J, Putranto EW, Ruma IMW, Sumardika IW, Youyi C, Suzawa K, Yamamoto H, Soh J, Tomida S, Sakaguchi Y, Saito K, Iioka H, Huh N, Toyooka S, Sakaguchi M. Active secretion of dimerized S100A11 induced by the peroxisome in mesothelioma cells. Cancer Microenviron. 2016; 9(2–3):93–105.

12. Sakaguchi M, Huh NH. S100A11, a dual growth regulator of epidermal keratinocytes. Amino Acids 2011;41(4): 797–807.
13. Sakaguchi M, Miyazaki M, Inoue Y, Tsuji T, Kouchi H, Tanaka T, Yamada H, Namba M. Relationship between contact inhibition and intranuclear S100C of normal human fibroblasts. J Cell Biol. 2000;149(6):1193–206.
14. Sakaguchi M, Miyazaki M, Sonegawa H, Kashiwagi M, Ohba M, Kuroki T, Namba M, Huh NH. PKCalpha mediates TGFbeta-induced growth inhibition of human keratinocytes via phosphorylation of S100C/A11. J Cell Biol. 2004;164(7):979–84.
15. Sakaguchi M, Miyazaki M, Takaishi M, Sakaguchi Y, Makino E, Kataoka N, Yamada H, Namba M, Huh NH. S100C/A11 is a key mediator of Ca(2+)-induced growth inhibition of human epidermal keratinocytes. J Cell Biol. 2003;163(4):825–35.
16. Sakaguchi M, Sonegawa H, Murata H, Kitazoe M, Futami J, Kataoka K, Yamada H, Huh NH. S100A11, an dual mediator for growth regulation of human keratinocytes. Mol Biol Cell 2008;19(1):78–85.
17. Sato H, Sakaguchi M, Yamamoto H, Tomida S, Aoe K, Shien K, Yoshioka T, Namba K, Torigoe H, Soh J, Tsukuda K, Tao H, Okabe K, Miyoshi S, Pass HI, Toyooka S. Therapeutic potential of targeting S100A11 in malignant pleural mesothelioma. Oncogenesis 2018;7(1):11.
18. Xiao MB, Jiang F, Ni WK, Chen BY, Lu CH, Li XY, Ni RZ. High expression of S100A11 in pancreatic adenocarcinoma is an unfavorable prognostic marker. Med Oncol. 2012;29(3):1886–91.
19. Sakaguchi M, Murata H, Yamamoto K, Ono T, Sakaguchi Y, Motoyama A, Hibino T, Kataoka K, Huh NH. TIRAP, an adaptor protein for TLR2/4, transduces a signal from RAGE phosphorylated upon ligand binding. PLoS One 2011;6(8):e23132.
20. Ohashi R, Miyazaki M, Fushimi K, Tsuji T, Inoue Y, Shimizu N, Namba M. Enhanced activity of cyclin A-associated kinase in immortalized human fibroblasts. Int J Cancer 1999;82(5):754–8.
21. Takamatsu H, Yamamoto KI, Tomonobu N, Murata H, Inoue Y, Yamauchi A, Sumardika IW, Chen Y, Kinoshita R, Yamamura M, Fujiwara H, Mitsui Y, Araki K, Futami J, Saito K, Iioka H, Winarsa Ruma IM, Putranto EW, Nishibori M, Kondo E, Yamamoto Y, Toyooka S, Sakaguchi M. Extracellular S100A11 plays a critical role in spread of the fibroblast population in pancreatic cancers. Oncol Res. 2019. [E-pub ahead of print]
22. Kinoshita R, Sato H, Yamauchi A, Takahashi Y, Inoue Y, Sumardika IW, Chen Y, Tomonobu N, Araki K, Shien K, Tomida S, Torigoe H, Namba K, Kurihara E, Ogoshi Y, Murata H, Yamamoto KI, Futami J, Putranto EW, Winarsa Ruma IM, Yamamoto H, Soh J, Hibino T, Nishibori M, Kondo E, Toyooka S, Sakaguchi M. exSSSRs (extracellular S100 soil sensor receptors)-Fc fusion proteins work as prominent decoys to S100A8/A9-induced lung tropic cancer metastasis. Int J Cancer 2019;144(12):3138–45.
23. Futami J, Atago Y, Azuma A, Putranto EW, Kinoshita R, Murata H, Sakaguchi M. An efficient method for the preparation of preferentially heterodimerized recombinant S100A8/A9 coexpressed in Escherichia coli. Biochem Biophys Rep. 2016;6:94–100.
24. Sakaguchi M, Watanabe M, Kinoshita R, Kaku H, Ueki H, Futami J, Murata H, Inoue Y, Li SA, Huang P, Putranto EW, Ruma IM, Nasu Y, Kumon H, Huh NH. Dramatic increase in expression of a transgene by insertion of promoters downstream of the cargo gene. Mol Biotechnol. 2014;56(7):621–30.
25. Kinoshita R, Sato H, Yamauchi A, Takahashi Y, Inoue Y, Sumardika IW, Chen Y, Tomonobu N, Araki K, Shien K, Tomida S, Torigoe H, Namba K, Kurihara E, Ogoshi Y, Murata H, Yamamoto KI, Futami J, Putranto EW, Ruma IMW, Yamamoto H, Soh J, Hibino T, Nishibori M, Kondo E, Toyooka S, Sakaguchi M. Newly developed anti-S100A8/A9 monoclonal antibody efficiently prevents lung tropic cancer metastasis. Int J Cancer 2019;145(2):596–75.
26. Ruma IM, Putranto EW, Kondo E, Murata H, Watanabe M, Huang P, Kinoshita R, Futami J, Inoue Y, Yamauchi A, Sumardika IW, Youyi C, Yamamoto K, Nasu Y, Nishibori M, Hibino T, Sakaguchi M. MCAM, as a novel receptor for S100A8/A9, mediates progression of malignant melanoma through prominent activation of NF-κB and ROS formation upon ligand binding. Clin Exp Metastasis 2016;33(6):609–27.
27. Hibino T, Sakaguchi M, Miyamoto S, Yamamoto M, Motoyama A, Hosoi J, Shimokata T, Ito T, Tsuboi R, Huh NH. S100A9 is a novel ligand of EMMPRIN that promotes melanoma metastasis. Cancer Res. 2013;73(1): 172–83.
28. Sakaguchi M, Yamamoto M, Miyai M, Maeda T, Hiruma J, Murata H, Kinoshita R, Winarsa Ruma IM, Putranto EW, Inoue Y, Morizane S, Huh NH, Tsuboi R, Hibino T. Identification of an S100A8 receptor neuroplastin-β and its heterodimer formation with EMMPRIN. J Invest Dermatol. 2016;136(11):2240–50.
29. Yan HH, Jiang J, Pang Y, Achyut BR, Lizardo M, Liang X, Hunter K, Khanna C, Hollander C, Yang L. CCL9 induced by TGFbeta signaling in myeloid cells enhances tumor cell survival in the premetastatic organ. Cancer Res. 2015;75(24):5283–98.
30. Liu Z, Zhang J, Gao Y, Pei L, Zhou J, Gu L, Zhang L, Zhu B, Hattori N, Ji J, Yuasa Y, Kim W, Ushijima T, Shi H, Deng D. Large-scale characterization of DNA methylation changes in human gastric carcinomas with and without metastasis. Clin Cancer Res. 2014;20(17): 4598–612.
31. Wang YC, Yu SQ, Wang XH, Han BM, Zhao FJ, Zhu GH, Hong Y, Xia SJ. Differences in phenotype and gene expression of prostate stromal cells from patients of varying ages and their influence on tumour formation by prostate epithelial cells. Asian J Androl. 2011;13(5):732–41.
32. Pal SK, Nguyen CT, Morita KI, Miki Y, Kayamori K, Yamaguchi A, Sakamoto K. THBS1 is induced by TGFB1 in the cancer stroma and promotes invasion of oral squamous cell carcinoma. J Oral Pathol Med. 2016; 45(10):730–9.
33. Stokes A, Joutsa J, Ala-Aho R, Pitchers M, Pennington CJ, Martin C, Premachandra DJ, Okada Y, Peltonen J, Grenman R, James HA, Edwards DR, Kahari VM. Expression profiles and clinical correlations of degradome components in the tumor microenvironment of head and neck squamous cell carcinoma. Clin Cancer Res. 2010; 16(7):2022–35.
34. Tanaka N, Yamada S, Sonohara F, Suenaga M, Hayashi M, Takami H, Niwa Y, Hattori N, Iwata N, Kanda M, Tanaka C, Kobayashi D, Nakayama G, Koike M, Fujiwara M, Fujii T, Kodera Y. Clinical implications of lysyl oxidase-like protein 2 expression in pancreatic cancer. Sci Rep. 2018;8(1):9846.

35. Eliopoulos AG, Dumitru CD, Wang CC, Cho J, Tsichlis PN. Induction of COX-2 by LPS in macrophages is regulated by Tpl2-dependent CREB activation signals. EMBO J. 2002;21(18):4831–40.

36. Xie C, Xu X, Wang X, Wei S, Shao L, Chen J, Cai J, Jia L. Cyclooxygenase-2 induces angiogenesis in pancreatic cancer mediated by prostaglandin E2. Oncol Lett. 2018; 16(1):940–8.